

**DEEP REACTIVE-ION ETCHING DEVELOPMENT WITH THE BOSCH  
PROCESS**

An Undergraduate Research Scholars Thesis

by

MARCELO PIER

Submitted to the LAUNCH: Undergraduate Research office at  
Texas A&M University  
in partial fulfillment of requirements for the designation as an

UNDERGRADUATE RESEARCH SCHOLAR

Approved by  
Faculty Research Advisor:

Dr. Arum Han

May 2022

Major:

Electrical Engineering

Copyright © 2022. Marcelo Pier.

## **RESEARCH COMPLIANCE CERTIFICATION**

Research activities involving the use of human subjects, vertebrate animals, and/or biohazards must be reviewed and approved by the appropriate Texas A&M University regulatory research committee (i.e., IRB, IACUC, IBC) before the activity can commence. This requirement applies to activities conducted at Texas A&M and to activities conducted at non-Texas A&M facilities or institutions. In both cases, students are responsible for working with the relevant Texas A&M research compliance program to ensure and document that all Texas A&M compliance obligations are met before the study begins.

I, Marcelo Pier, certify that all research compliance requirements related to this Undergraduate Research Scholars thesis have been addressed with my Research Faculty Advisors prior to the collection of any data used in this final thesis submission.

This project did not require approval from the Texas A&M University Research Compliance & Biosafety office.

# TABLE OF CONTENTS

	Page
ABSTRACT.....	1
DEDICATION.....	3
ACKNOWLEDGEMENTS.....	4
NOMENCLATURE.....	5
CHAPTERS	
1. INTRODUCTION.....	6
1.1 Etching.....	6
1.2 Deep Reactive-Ion Etching.....	7
2. METHODS.....	9
2.1 Sample/Substrate Preparation.....	9
2.2 Photolithography.....	10
2.3 Thin Film Deposition.....	16
2.4 Thermal Oxidation.....	19
2.5 Wet Etching.....	21
2.6 The Bosch Process.....	23
2.7 Scanning Electron Microscopy.....	26
3. RESULTS.....	28
3.1 Test Sample Etch Mask Results.....	28
3.2 Etch Mask Thickness.....	30
3.3 Effect of Inductively Coupled Plasma Power.....	31
3.4 Effect of CHF <sub>3</sub> Gas Flow Rate.....	34
4. CONCLUSIONS.....	38
4.1 Summary.....	38
4.2 Next Steps.....	38
REFERENCES.....	40

# ABSTRACT

Deep Reactive-Ion Etching Development with the Bosch Process

Marcelo Pier  
Department of Electrical and Computer Engineering  
Texas A&M University

Research Faculty Advisor: Dr. Arum Han  
Department of Electrical and Computer Engineering  
Texas A&M University

The Bosch process is a type of deep reactive-ion etching (DRIE) of silicon. It is a type of plasma etching, or dry etching, that uses physical and chemical processes to etch the surface of a silicon sample. Due to its highly desirable results, this process is used in several applications, such as nanoscale MOSEFTS, microelectromechanical systems, and micro-optics.

This process is unique because it switches between process gases or plasma chemistries to create a fluorine base for etching while also creating a carbon layer for sidewall protection. The process cycles between etching with fluorine and depositing a carbon layer coating, which is a process known as passivation.

During standard reactive-ion etching (RIE), there is possibility of rough sidewalls, a low aspect ratio, and growth of silicon grass at the bottom of the feature trench, some of which can be as tall as the etched feature itself. Thus, the Bosch process is a highly effective process that results in higher etch rates than regular RIE. In addition, it enables selectivity and anisotropy and eliminates the possibility of silicon grass formation in etched trenches. The most desirable

aspects of this process are its abilities to etch while maintaining smooth sidewalls and produce high-aspect-ratio features with vertical sidewalls.

The Bosch process for DRIE will be implemented on an Oxford Plasmalab100 ICP RIE machine. Throughout development, thin film deposition, thermal oxidation, photolithography, silicon dicing, wet etching, and cross-sectional scanning electron microscopy processes will be used.

## **DEDICATION**

*To my family, who have always been there to support me through everything I undertake.*

## **ACKNOWLEDGEMENTS**

### **Contributors**

Thank you to Dr. Arum Han for his support and advising of this thesis and allowing me to conduct my research at the AggieFab Nanofabrication Facility.

Thank you to Dr. Sandra Malhotra for her guidance and wisdom throughout the time I have been employed at AggieFab and throughout my research for this thesis.

Thank you to Jung Hwan Woo for always providing helpful feedback and knowledge throughout my time at AggieFab and especially for helping direct the goal of this research.

Thank you to Megan Makela for offering her time to make sure I understood complex topics and ran procedures correctly, as well as offer much needed moral support.

Thank you to all others who have helped me and given me new friendships throughout my time at AggieFab: Don Marek, Ted Wangenstein, Christopher Karber, Mitchell Roselius, Elijah Colter, Bryce Prucha, Ruben Carreon, Bailey Faulk, and Hanna Prichard.

Finally, thank you to my mom and dad for their unceasing support.

The data analyzed/used for this thesis were provided by AggieFab Nanofabrication Facility. The analyses depicted in this thesis were conducted in part by AggieFab staff members and these data are unpublished.

All other work conducted for the thesis was completed by the student independently.

### **Funding Sources**

This Undergraduate Research received no funding.

## NOMENCLATURE

BOE	Buffered Oxide Etchant
Cr	Chromium
DI	Deionized
DRIE	Deep reactive-ion etching
H <sub>2</sub> O	Water
H <sub>2</sub> O <sub>2</sub>	Hydrogen Peroxide
H <sub>2</sub> SO <sub>4</sub>	Sulfuric Acid
ICP	Inductively-coupled plasma
ICPP	Inductively-coupled plasma power
IPA	Isopropyl Alcohol
MIF	Metal ion free
PVD	Physical vapor deposition
RIE	Reactive-ion etching
RPM	Revolutions per minute
SEM	Scanning electron microscope
Si	Silicon
SiO <sub>2</sub>	Silicon dioxide



# 1. INTRODUCTION

## 1.1 Etching

During nanofabrication, etching is the process of removing certain areas, like thin films of materials, from a sample or substrate. However, during etching, specific areas are not etched if there is an etch mask present. An etch mask is resistant to the etching procedure and can be composed of a variety of different materials. Photoresists, which are ultraviolet (UV)-sensitive materials, can be applied to a sample using photolithography. Metals, such as chromium (Cr), can be used as an etch mask and deposited on a material using thin film deposition techniques. Thermally grown films, such as silicon dioxide ( $\text{SiO}_2$ ), can be used as etch masks as well.

There are two types of etch methods: wet etching and dry etching. To determine which type to use, it is important to consider the etching characteristics. These include isotropy and anisotropy. Isotropic etching has a constant etching rate along all directions, which means that the properties of a material on a substrate are independent of the direction. On the other hand, anisotropic etching only etches along a certain direction of a material, which means that this method is dependent on the direction. Another important factor is the selectivity. Selectivity is the ratio of the etch rate of the mask to the etch rate of the material being etched.

As mentioned before, there are dry etching and wet etching methods. Dry etching is a type of plasma etching that utilizes ion bombardment on a substrate to remove a masked pattern. Usually, these ions are from a process gas, like oxygen or fluorine. Unlike some wet etching methods, dry etching can be isotropic or anisotropic, since both are possible. Reactive-ion etching (RIE) is a form of dry etching where a substrate is placed inside a chamber with various

process gases. These process gases create a plasma within the chamber by using a radio frequency (RF) power source that breaks gas molecules into ions.

Wet etching is a more basic process that uses a liquid chemical, usually with a chelating agent, to break down materials. Wet etching, also known as chemical etching, is done by submerging a sample or wafer in an etchant solution container. This way, the chemical dissolves the material being etched. Different etch mask materials use different types of wet etching chemicals. For example, for a metal etch mask, such as a chromium, a chromium etchant can be used to chemically etch the substrate. Other common wet etching chemicals are buffered oxide etchant (BOE) for silicon dioxide (SiO<sub>2</sub>) etch masks [4].

## **1.2 Deep Reactive-Ion Etching**

In the field of silicon etching, which is prevalent in semiconductor fabrication, there are two different types of deep reactive-ion etching (DRIE) processes. There is a cryogenic deep reactive-ion etch and the Bosch process. Both of these are etching procedures that use plasma etching, which is a type of dry etching. Dry etches use physical and chemical effects to etch the surface of a sample or substrate, which is usually a silicon wafer [1].

During cryogenic DRIE, the temperature of the silicon substrate is a key component. This is because the temperature has a direct impact on the sidewall profiles of the sample. Liquid nitrogen is connected directly to the chamber and enables cooling of the stage and silicon wafer. The temperature of the stage and the substrate are on the order of minus hundreds of degrees celsius. At these temperatures, the condensation creates a pseudo-passivation layer, which is similar to the carbon passivation layer that the Bosch process utilizes [1].

The Bosch DRIE method switches between different process gases/plasma chemistries to provide a base of fluorine for the etching while also protecting the sidewall with a carbon layer.

A complete etching process switches between etching with a fluorine-based plasma chemistry and depositing a sidewall passivation (coating) with the goal of creating deep, vertical etch profiles (i.e., high aspect ratio trenches) [2]-[3].

The Bosch process is a more favorable etch procedure for those seeking DRIE than cryogenic etching because the results tend to be more desirable. For example, cryogenic etching tends to create silicon grass formations at the bottom of etched features, while the Bosch process produces features with a smooth bottom.

## 2. METHODS

### 2.1 Sample/Substrate Preparation

The sample preparation involved a cleanse of the substrates that were to be used for development of the etching process. An ideal substrate is one that is free of any particles, especially organic materials, that could have an adverse impact on the development in the subsequent subsystems.

The preparation of the substrates was composed of two main procedures. The substrates, also referred to as the samples, were 2-inch silicon wafers. These wafers were first cleansed using a solvent clean. The solvent clean used here sprayed the surface of the wafer using isopropyl alcohol (IPA), submerged the wafer in a bath of acetone, and finally rinsed the surface of the wafer using deionized water (DI).

The solvent bath was then followed by a piranha acid clean. Piranha acid is a solution that contains three parts sulfuric acid ( $H_2SO_4$ ) and one part hydrogen peroxide ( $H_2O_2$ ). This acid is highly volatile and ensures that any/all materials, including organic materials, are removed from the surface of the silicon wafer.

The Nikon Eclipse LV150N optical microscope in AggieFab can reach 100x magnification and ultimately allows for checking to see if any particles survived both the solvent and piranha acid cleans. Considering that piranha solutions react with organic materials, the surface of the wafers should be completely clean, especially if they are placed in an enclosed wafer cassette immediately after the piranha acid cleanse is complete.

## 2.2 Photolithography

Photolithography is the procedure where a photoresist is applied to the surface of a silicon wafer. Photoresists are UV-sensitive materials that cover the entirety of a silicon wafer by using a photoresist spin coater. After the photoresist is applied, it is patterned using a mask aligner, which exposes the photoresist to a specific dosage of UV light and degrades the photoresist that was unmasked, thus resulting in a pattern. Figure 1 shows a cross-sectional sideview of the photoresist layer applied to a silicon wafer.



*Figure 1: Test sample photoresist layer*

The application of a thin layer of AZ<sup>®</sup> 5214 E-IR positive photoresist to the surface of the sample was done using a BIDTEC SP100 Spin Coater. This tool uniformly spreads the photoresist on the sample. The recipe parameters determine the final thickness of the photoresist on the sample. The spin coater is shown in Figure 2, and the recipe parameters are shown in Table 1. The recipe parameters were experimentally determined to result in a specific final thickness. When the parameters shown in Table 1 were used, the film of photoresist applied to the substrate was consistently in the range from 1.35-1.45 microns ( $\mu\text{m}$ ). The recipe parameters provided in Table 1 resulted in an average photoresist final thickness of 1.4  $\mu\text{m}$ . This was a direct result of a Speed 2 value of 4000 revolutions per minute (rpm). The photoresist thickness was measured using the Ocean Optics NanoCalc deep UV (DUV) spectroscopic thin film measurement profilometer. This tool measures the thickness of thin films by utilizing spectroscopic reflectometry (light reflection). Essentially, it is an excellent tool for measuring the

final thickness of photoresist. All Speed 2 values lower than 4000 rpm resulted in layers thicker than 1.4 microns; thus, 4000 rpm was used to achieve this result.



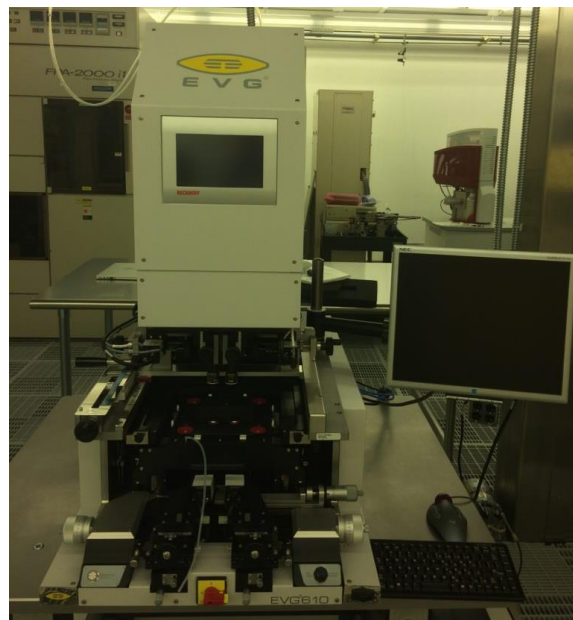
Figure 2: BIDTEC SP100 spin coater

Table 1: Spin coater recipe parameters

Parameter	Value
Speed 1	500 rpm
Time to speed 1	10 s
Time at speed 1	5 s
Speed 2	4000 rpm
Time to speed 2	5 s
Time at speed 2	45 s
Time to 0 rpm	5 s

Once 1.4 microns of photoresist was obtained, the sample was soft baked on a hotplate at 120° C for 60 seconds and then taken directly to the mask aligner.

The final thickness of the samples was input into the recipe for the mask aligner, where a dosage of  $100 \text{ mJ/cm}^2$  was determined to be ideal. This was concluded because the photoresist patterns on the wafers were underexposed with dosages under 100 and overexposed with dosages above 100. These dosages were determined specifically for AZ<sup>®</sup> 5214 E-IR positive photoresist. The EVG 610 double-sided mask aligner exposes the photoresist on samples to a specified UV light dosage and under a specific patterning mask. Patterning masks block UV light in certain areas, only allowing light to transmit through the openings in the mask pattern so that those specific areas of photoresist on the surface of the wafer are not dissolved. This creates a pattern on the substrate that contains the features from that patterning mask. Once it was exposed, the photoresist was patterned and ready to be taken out of the mask aligner. The mask aligner is shown in Figure 3, and the recipe parameters for it are shown in Table 2.



*Figure 3: EVG 610 double-sided mask aligner*

Table 2: Mask aligner recipe parameters

Parameter	Value
Soft Contact Distance	30 $\mu\text{m}$
Photoresist Thickness	1.4 $\mu\text{m}$
UV Light Dosage	100 $\text{mJ}/\text{cm}^2$

Directly after being removed from the mask aligner, the samples were submerged in AZ<sup>®</sup> 726 metal-ion free (MIF) developer for 45 seconds and then rinsed using DI water. Finally, the samples were placed in an oven at 160° C for 10:00 minutes. The result after utilizing both the spin coater and the mask aligner was a silicon wafer sample with a patterned and uniform layer of photoresist. Figure 4 and 5 both show microscopic images of the pattern at different magnifications. The pattern that was used was from a standard calibration mask available at the AggieFab Nanofabrication Facility.

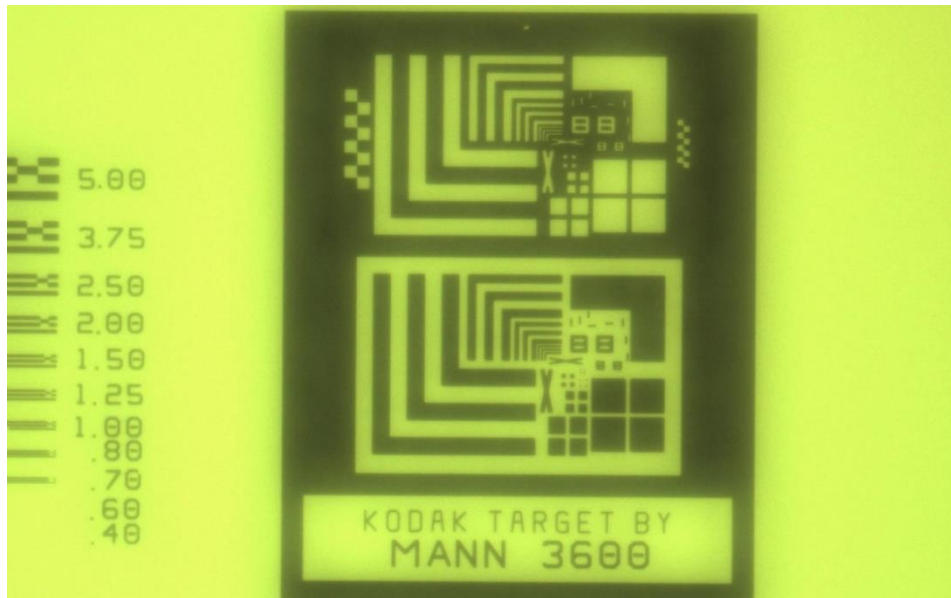


Figure 4: AggieFab standard calibration mask (20x)



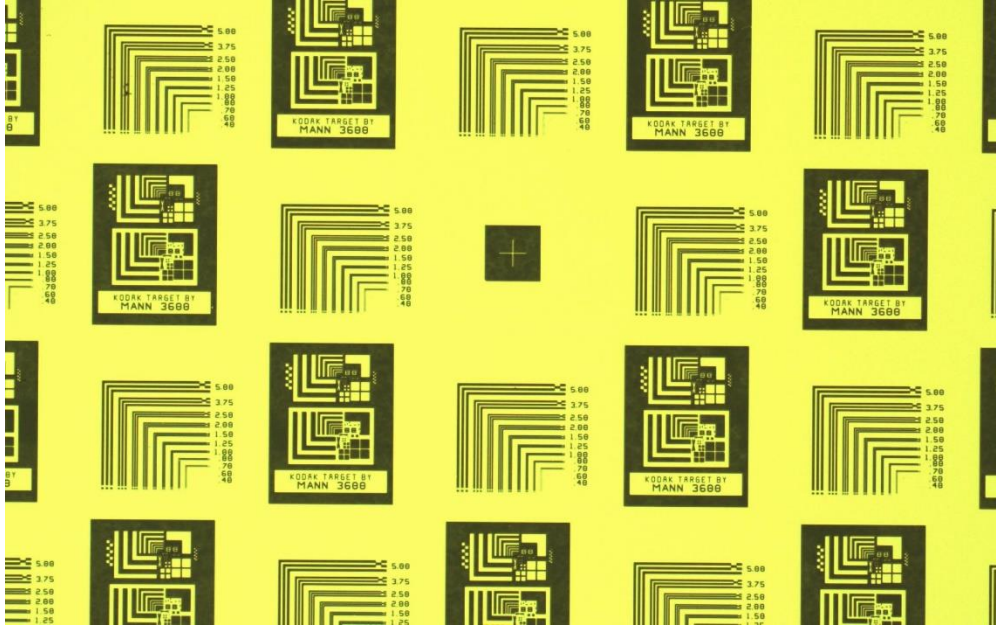
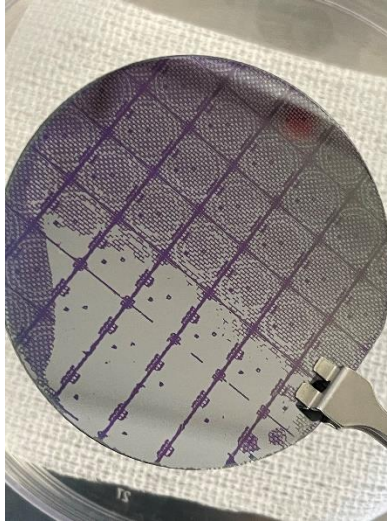


Figure 5: AggieFab standard calibration mask (5x)

Figure 4 shows a single feature on the pattern at 20x magnification that has both a brightfield and a darkfield pattern. The patterns were the same, but they were the inverse of each other. This is important to note considering that later in the sample process, the etch mask for sample 2 was the inverse of the etch masks from samples 1 and 3. This did not have an adverse effect on analyzing the resulting etches because this pattern had both brightfield and darkfield patterns, so the area of etch that was analyzed was different, but the result was the same.

Figure 5 is zoomed out at 5x magnification and shows an array of repeating patterns. The black squares with patterns inside are from Figure 4, and the L-shaped arrays adjacent to those are patterns that can be used to analyze the resulting etches. The numbers next to them represent the variable width and spacing and are in the order of microns ( $\mu\text{m}$ ).

Figure 6 shows a photolithography test run which resulted in an underexposed pattern on it. The photoresist mask is uneven and is clearly missing features. Figure 7 shows a perfectly exposed wafer with an even mask and all features present.



*Figure 6: Underexposed photoresist pattern*



*Figure 7: Correctly exposed photoresist pattern*

### 2.3 Thin Film Deposition

Thin film deposition is a type of physical vapor deposition (PVD) that is used for the application of materials on the surfaces of substrates. This process focuses on applying those materials using an electron beam to melt and ultimately evaporate said material onto a sample. Thin film deposition is generally for metallic materials. Figure 8 shows a cross-sectional view of the chromium, a metallic layer, applied to the silicon wafer. It should be mentioned that chromium cannot be patterned like photoresist using UV light. Therefore, to create an etch mask of a metal, photoresist is applied as a first layer and patterned, as previously stated. Then, the metallic layer is deposited on top, which takes the form of the patterned photoresist layer underneath it.

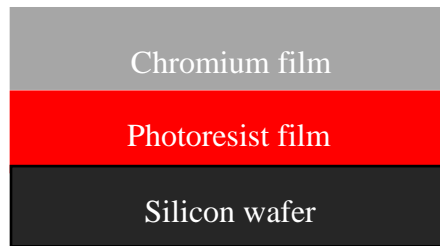


*Figure 8: Test sample photoresist + Cr layers*

The thin film deposition process specifically utilized the Kurt J. Lesker PVD 75 electron beam evaporation (EBE or E-beam) tool. This tool specializes in the deposition of low-contamination films under a vacuum. The tool uses an electron beam to melt small pellets of metallic materials that are placed in a graphite crucible. The material evaporates inside the process chamber, ultimately covering the samples that are loaded inside. Chrome was the metallic material that was used herein because it is cheap and is straightforward to use. Figure 9 shows the Lesker PVD 75 E-beam tool, and Table 3 shows the recipe parameters used on this machine.



Figure 9: Lesker PVD 75 electron beam evaporator

Table 3: E-beam recipe parameters

Parameter	Value
PC Pressure	$5 \times 10^{-6}$ Torr
Deposition Rate	0.2 nm/s
Power 1	0.7 %
Power 2	1.2 %
Crystal Monitor Quality	> 90%
Platen Rotation Speed	20 rpm
Final Thickness	100 nm

The process chamber (PC) was under vacuum with a pressure of  $5 \times 10^{-6}$  Torr. The power ramped up to 0.7% to heat the material, and then, it ramped up to 1.2% to evaporate it. From

there, the power increased or decreased depending on if the desired deposition rate was too low or too high, respectively. Then, the power stabilized, and the material was deposited on the samples in the chamber. The final thickness was set at 100 nm at a rate of 0.2 nm/s.

The platen rotation speed is the speed, in rpm, at which the stage rotates. The platen, or stage, is a flat platform onto which samples are mounted using Kapton tape, which is a heat resistant tape. The platen hung upside down with the samples facing down. The deposition material was evaporated upwards and coated the platen. This stage rotated at 20 rpm because it was shown to produce the best layer uniformity from edge to edge of the silicon wafer.

The E-beam crystal monitor is an instrument used to measure the deposition rate of the evaporating material and calculates the final thickness of the material inside the chamber. It calculates this thickness even through ramping up and down of the power; however, there are two shutters in the chamber that block deposition from being applied to the sample surface. The crystal has a quality percentage attached to it. The higher the percentage, the more accurate the calculated thickness is. Although a fairly accurate means of determining film thickness, a profilometer was used to verify the true thickness of the newly deposited film.

The Bruker DektakXT Surface Profiler is a profilometer, much like the Ocean Optics, but it measures the step height of films using a stylus instead of using spectroscopic reflectometry. This is much better suited to the measurement of metallic thin films, which is why it was used over the Ocean Optics spectrometer. This tool measured the thickness of the thin films after deposition using the E-beam tool. The measured thin film thickness from the Dektak was then cross-referenced with the calculated thickness from the E-beam tool's crystal monitor. If a margin of error of more than 10% was found between the two final thickness measurements, the sample was wiped and reprocessed; however, this occurrence was extremely rare.

## 2.4 Thermal Oxidation

The thermal oxidation process grows a film of silicon dioxide ( $\text{SiO}_2$ ) on a silicon substrate with excellent uniformity. There are two types of oxidation types, namely, wet and dry oxidation. Wet oxidation produces  $\text{SiO}_2$  using water vapor, and dry oxidation produces it using oxygen. This test sample utilized the wet oxidation growth procedure and resulted in the growth of 500 nm of  $\text{SiO}_2$  on top of a silicon wafer. Figure 10 shows the layers that resulted from this procedure.

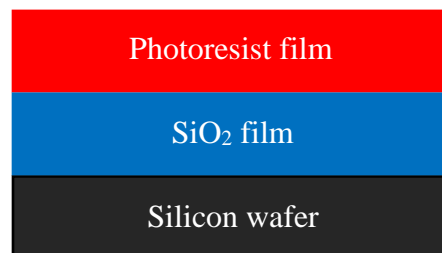


*Figure 10: Test sample photoresist +  $\text{SiO}_2$*

Thermal oxidation was performed using the Minibrute oxidation/anneal furnaces. The Minibrutes are atmospheric furnaces that allow for thermal oxidation using either wet or dry oxidation. Several process gases are available for use, such as oxygen and nitrogen. In addition, there was a steam generator, also known as the bubbler, which is essential for performing a wet oxidation procedure. The wafer carriers were made of quartz, can withstand extreme heat, and held up to 25 samples. The Minibrutes have three tubes that act as different kinds of furnaces. Tube 1 is mainly for metal anneals and sintering processes. Tube 2 and 3 are both for oxidation and have the steam generator available for wet oxidation. Figure 11 shows the Minibrute oxidation/anneal furnace, which is used for thermal oxidation, and Table 4 shows the recipe parameters.



Figure 11: Minibrute oxidation/anneal furnaces

Table 3: Minibrute recipe parameters

Parameter	Value
Oxidation Type	Wet
Bubbler Prep Time	60 min
Temp Ramp Up	10°C/min
Quartz Tube Heating Temp	1100°C
Gas	99.999% N <sub>2</sub>
Cooling Time	15 min
Final Thickness	500 nm

As previously stated, wet oxidation was used, which means that water vapor was introduced into the chamber where the samples were placed. The reason this procedure used wet oxidation is because it produced a “sacrificial oxide”, which means that it was removed later. The bubbler was prepared for an hour beforehand to ensure an adequate amount of steam would

be generated. After an initial heat acclimation step, which allowed wafers to slowly warm up in the furnace to prevent thermal shock, the nitrogen supply was turned off and the bubbler was connected to the chamber, or tube, of the furnace. While the tube was being heated to 1100° C (standard furnace temperature) at a rate of 10°C/min, pure nitrogen (N<sub>2</sub>), which is a process gas attached to the furnace tube, was flowing throughout the tube. There should be no other source of oxygen molecules in the tube during the procedure, because if there was, it could hinder the SiO<sub>2</sub> film growth. After 500 nm of silicon dioxide was grown, the bubbler was disconnected so that no more silicon dioxide grew, and the nitrogen flow was turned on again.

It should be noted that test sample 2 had photoresist as the first layer, then chromium was applied on top. On the other hand, test sample 3 had SiO<sub>2</sub> grown first, then photoresist was applied. The order of layers was different in these cases because photoresist would evaporate in the Minibrute furnaces and contaminate the furnace tube; thus, photoresist was applied after the SiO<sub>2</sub> was grown on the sample.

Like with photolithography, the thin film on test sample 3 was measured using the Ocean Optics spectrometer. The Ocean Optics has a calibration wafer that has thermally grown SiO<sub>2</sub> on it, which allows for highly accurate measurements of SiO<sub>2</sub>. The measurements for the Minibrute process were extremely close to 500 nm consistently and proved to be extremely uniform from edge to edge of the samples.

## **2.5 Wet Etching**

The wet etching process removes material from specific areas using liquid chemicals. There were three test samples created that required the use of wet etching to finalize the etch masks.



The first test sample comprised a thin film of photoresist. After the sample was coated with photoresist, it was placed in the mask aligner for patterning. However, after it was exposed to UV light, the pattern was not visible. Instead, the freshly degraded photoresist needed to be removed using AZ<sup>®</sup> 726 metal-ion free (MIF) developer. After the wafer was submerged in this developer, the degraded photoresist etched off and the pattern was visible.

The time that the sample is submerged in the liquid chemical for development of the pattern is an important factor in correctly creating an etch mask. There is a possibility that the photoresist can be over- or underdeveloped. For correct development of the mask, the wafers spent an average of 45 seconds in the solution. At times, it was apparent that the etch mask was underdeveloped, as previously shown in Figure 6. When it was not as apparent, the Nikon Eclipse optical microscope was used to examine the pattern and verify that the etch mask was correctly developed. If underdeveloped, the sample was submerged in the etchant at 5 second intervals and verified at each interval using the Nikon Eclipse. However, if the pattern was overdeveloped, it was completely removed from the sample using AZ<sup>®</sup> 400T photoresist stripper. The samples were submerged in the photoresist stripper which was heated using a hot plate set to 85 °C. After it was taken out, a solvent clean was performed, and the photoresist was reapplied to the sample by undergoing the entire photolithography procedure again. This development process was common to all three test samples, since they all used photoresist.

For test sample 2, the chromium layer covered the entire patterned photoresist layer, which means that there were certain areas where chromium was directly on top of the photoresist, and other areas where it was directly on top of the wafer (Cr-Si interface). This is because the photoresist layer was already patterned, and the chromium layer applied on top duplicated that pattern. Since the etch mask, in this case chromium, was on top of the photoresist

layer, a procedure known as lift-off was used to finalize the pattern. It should be noted that lift-off is not necessarily etching but rather removal of material in a different way. Nevertheless, the sample is still submerged in a liquid chemical during this process. Just like in the first test sample, AZ<sup>®</sup> 400T photoresist stripper was used to remove all the photoresist. While doing so, the chromium on top of that photoresist was removed as well. The result was a wafer with a patterned chromium etch mask.

For test sample 3, the photoresist pattern was applied after the SiO<sub>2</sub> film was thermally grown. Therefore, etching was used rather than lift-off, since the etch mask was removed in this step. The photoresist was patterned and the degraded photoresist was etched away, leaving specific areas where SiO<sub>2</sub> was exposed underneath the photoresist layer. The wet etching chemical in this case was buffered oxide etchant (BOE). When the wafer was submerged in this chemical, all the SiO<sub>2</sub> that was exposed underneath the photoresist mask was degraded and etched away. The samples were submerged in BOE for 3:30 minutes. However, there was one more step needed for this test sample's etch mask to be complete. There was still photoresist on this test sample, so the procedure to etch away photoresist from test sample 3 was done with the same process as for test sample 1. The only difference is that the photoresist stripper was heated to 200 °C for a few minutes then ramped down to 130 °C. Afterwards the samples were taken out and dried, and the result was a patterned layer of SiO<sub>2</sub> on a silicon wafer.

## **2.6 The Bosch Process**

The Bosch process is an industry leading DRIE procedure that cycles between a deposition and passivation step. According to Oxford Instruments, SF<sub>6</sub> and C<sub>4</sub>F<sub>8</sub> are the etch and passivation gases, respectively, used to perform a Bosch DRIE procedure. A Bosch process recipe was created for the Oxford Plasmalab100 ICP RIE tool. An important distinction that

should be noted is that this recipe utilizes  $\text{CHF}_3$  as a passivation gas instead of the industry standard  $\text{C}_4\text{F}_8$ . Figure 12 shows the Oxford RIE and Figure 13 shows the recipe steps created for testing this process.



Figure 12: Oxford Plasmalab100 ICP RIE



Figure 13: Bosch Process Recipe Steps

The recipe calls for a stabilization of gases before beginning to cycle between the etch and passivation steps. As is shown, the etch and passivation steps will loop 20 times and end with a final etch to finish the process. This is important so that Si is exposed at the trench bottom instead of a passivation layer.

There are several parameters that make up the different steps of this recipe. For example, some parameters include gas flow (for both SF<sub>6</sub> and CHF<sub>3</sub>), ICP power, RF power, and pressure. Some of these parameters were held constant throughout etching, and some were variably changed to analyze their impacts on the DRIE. Table 4 shows constant parameters and Table 5 shows variable parameters.

*Table 4: DRIE Constant Parameters*

<b>Parameter</b>	<b>Value(s)</b>
SF <sub>6</sub> Gas Flow	100 SCCM
Chamber Pressure	30 mTorr
Chamber Temperature	10 °C
Helium Backside Cooling Pressure	5 mTorr
Helium Backside Cooling Gas Flow	35 SCCM
RF Power (Etch/Passivation)	30W/10W

*Table 5: DRIE Variable Parameters*

<b>Parameter</b>	<b>Values</b>
ICP Power	500/1000/2000 W
CHF <sub>3</sub> Gas Flow	30/60/90 SCCM

Before beginning a process, the liquid nitrogen (LN<sub>2</sub>) was opened so that low chamber temperatures can be reached, and then, the chamber was vented. The samples were mounted on top of a carrier wafer using Kapton tape and placed in the load lock. The load lock door was closed and the tool was pumped down to a pressure of  $5 \times 10^{-2}$  Torr. The Bosch process test recipe was loaded and ran. The total time for the recipe was around 15 minutes. After the process was complete, the wafer was automatically moved to the load lock. A visual check was performed through the viewing window to ensure the samples were safely taken out of the process chamber. Then the tool was vented to atmosphere to take the samples out. Several samples were used to test the effects of the changes in passivation gas flow and inductively coupled plasma power (ICPP) on the etching profiles. Selectivity and aspect ratio were analyzed for each etch mask.

## **2.7 Scanning Electron Microscopy**

A TESCAN MIRA3 scanning electron microscope (SEM) was used to analyze sample features after DRIE. The tool uses a secondary electron (SE) detector for analysis. Before placing the samples in the tool, they were cleaved using a wafer diamond scribe. This is done to cut features and create a cross-section for analysis. They were placed in the tool with the cleaved edge facing up towards the SEM column using a sample holder with carbon tape.

The chamber was then closed and pumped down to a pressure of  $9 \times 10^{-2}$  Pa, and the gun pressure was at  $10^{-8}$  Pa. The acceleration voltage was set at 10 kV for all imaging. The SEM was focused by adjusting the working distance, performing auto gun centering, column centering, and astigmatism correction. The TESCAN has scan speeds from 1 to 10. Images captured for analysis used a scan speed of 5. Greater scan speeds result in better image resolution; however, imaging takes significantly longer. Figure 14 shows the TESCAN SEM tool.

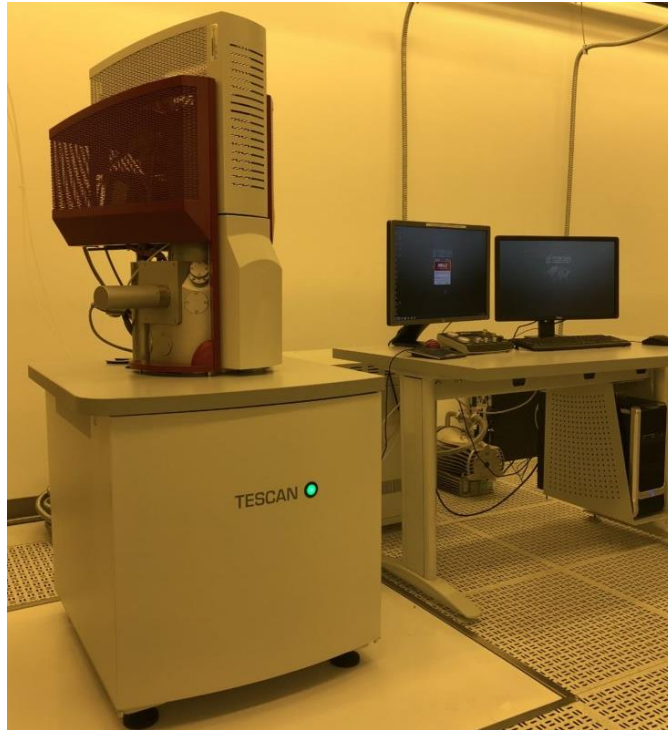


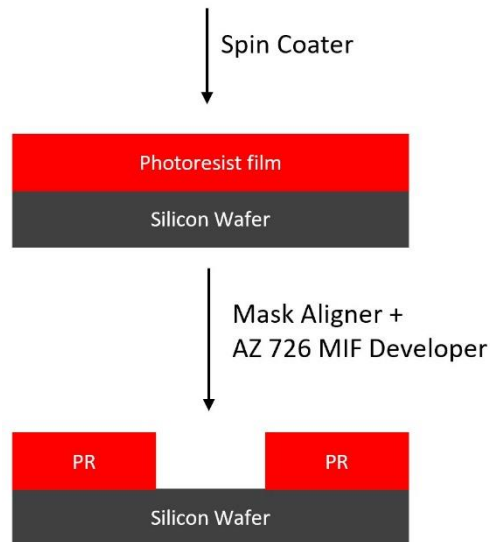
*Figure 14: TESCAN MIRA3 SEM*

### 3. RESULTS

#### 3.1 Test Sample Etch Mask Results

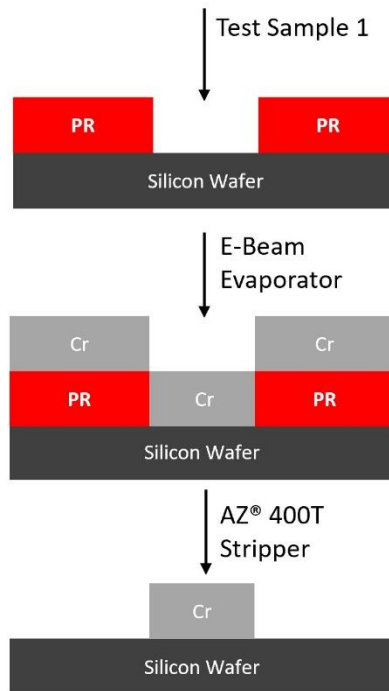
All three test samples were created for an analysis of DRIE characteristics, specifically, the selectivity and aspect ratio. To get a better understanding of these characteristics, the three test samples used different etch masks. The first test sample used photoresist, the second used chromium, and the third used SiO<sub>2</sub>.

Figure 12 shows a recap of the procedure that the first test sample underwent to achieve a photoresist etch mask. A cross-sectional view of the layers at different steps is shown after undergoing certain processes and/or procedures. Simply put, the spin coater applied photoresist, then the mask aligner along with the developer created and exposed a pattern in the photoresist. The result for the first test sample is shown, and this is how the sample appeared when it was ready to undergo DRIE.



*Figure 12: Test sample 1 procedure*

Figure 13 shows a cross-sectional view of the layers at each step for the second test sample. This procedure also included the procedure from test sample 1, and then, it was placed in the E-beam for chromium deposition. Finally, the photoresist stripper removed the photoresist with chromium on top and left a patterned chromium mask. This is an example of a lift-off procedure. As mentioned before, this etch mask was inverse that of the first and third test samples, but this was not an issue since the calibration mask from which this was patterned had both brightfield and darkfield patterns. The result of the second test sample is shown, and this is how the sample appeared when it was ready to undergo DRIE.



*Figure 13: Test sample 2 procedure*

Figure 14 shows a cross-sectional view of the layers at each step for the third test sample. This procedure started with thermally grown  $\text{SiO}_2$ , and then the sample underwent the photolithography process. Finally, BOE was used to etch the exposed  $\text{SiO}_2$ , and the photoresist stripper removed the remaining photoresist to leave a patterned  $\text{SiO}_2$  etch mask. This is an



example of a wet etching procedure. It used BOE, which is the etchant specifically made for oxide films.

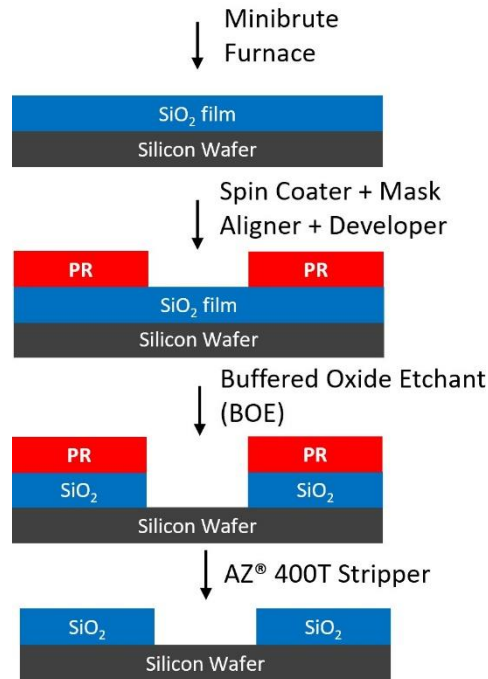


Figure 14: Test sample 3 procedure

### 3.2 Etch Mask Thickness

The three different etch masks used were AZ<sup>®</sup> 5214 E-IR positive photoresist, thermally grown SiO<sub>2</sub>, and electron beam evaporated chromium. Several samples were created, and their thicknesses were measured immediately after processing. Table 6 shows the average etch mask thicknesses across all samples created. These values were measured by the Bruker DektakXT Surface Profiler and the Ocean Optics NanoCalc deep UV (DUV) spectroscopic thin film measurement profilometer.

Table 6: Avg. Etch Mask Thickness

Etch Mask	Thickness
AZ <sup>®</sup> 5214 E-IR positive photoresist	1489 nm
SiO <sub>2</sub>	506.86 nm
Chromium (Cr)	106.7 nm

### 3.3 Effect of Inductively Coupled Plasma Power

The Oxford Plasmlab100 RIE used ICP created by electromagnetic induction. High frequency current in an RF induction coil allows for a circulating current to flow in a low pressure plasma. The main purpose of the ICP in this system is to increase etchants in the plasma. ICP was variably changed to determine its effect on aspect ratio and selectivity of the different etch mask samples. While keeping other parameters constant, the ICP was tested with 500 W, 1000 W and 2000 W. It is important to note that the maximum ICP the Oxford RIE is capable of is 2000 W.

Selectivity is the ratio of the target material's etch rate (in this case Si) to the etch rate of the etch mask material (PR, Cr, or SiO<sub>2</sub>). Using the TESCAN SEM, measurements were taken during imaging to determine the selectivity. The thickness of the remaining etch mask after etching was subtracted from the initial thickness of the etch mask to determine the amount of material etched. Then the Si etch depth was divided by this difference to give the selectivity value. Figure 15 shows the selectivity as a function of ICP. As the ICP increased, the selectivity of the Cr and SiO<sub>2</sub> samples increased. As for AZ 5214 E-IR, the selectivity remained steady regardless of changing ICP powers. Although the etch rates for the etch masks increased, the Si etch rate increased at a much higher rate, thus increasing selectivity overall.

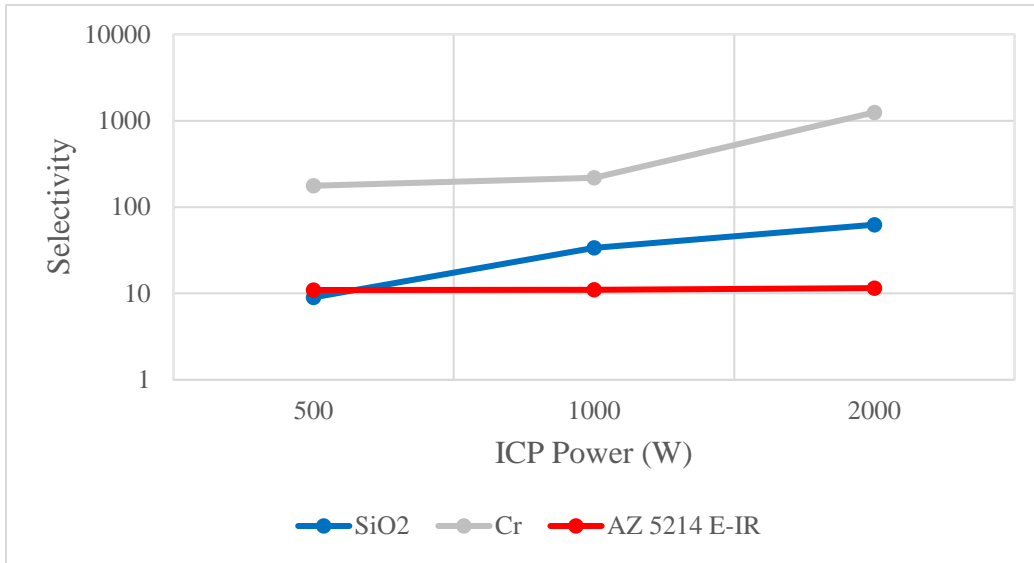


Figure 15: Selectivity vs. ICPP ( $CHF_3$  gas flow rate = 30 SCCM)

Figure 16 shows how measurements were taken during SEM imaging. In this case, the hard mask etched  $0.09\ \mu\text{m}$  while the Si etched  $5.63\ \mu\text{m}$ . Thus, the selectivity for this sample was about 62.5.

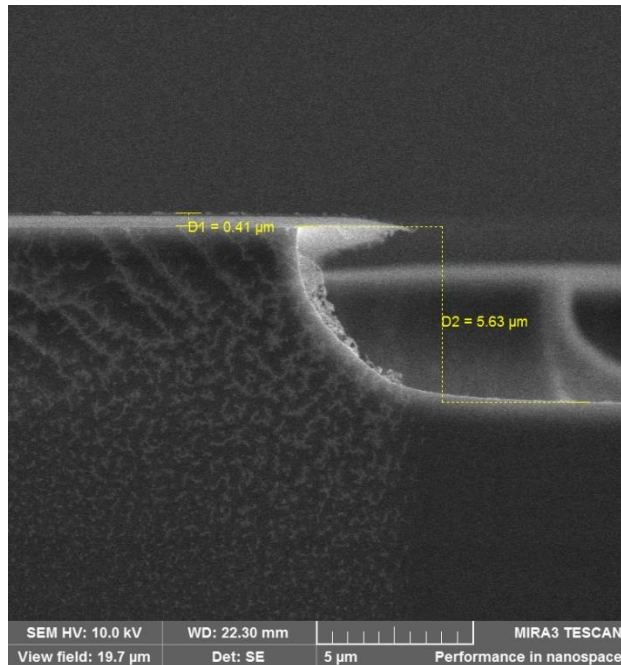


Figure 16: Etch mask selectivity measurements

The aspect ratio is the ratio between the depth and width of an etched feature. Like the selectivity, these measurements were taken using the TESCAN SEM. The depth of the etched feature was divided by the width of that feature to calculate its aspect ratio. Figure 17 shows the aspect ratio as a function of ICPP. Aspect ratio increased regardless of an increase in horizontal etching on the sidewalls for greater ICPP. For all etch masks tested, there was a positive correlation between the aspect ratio and the ICPP.

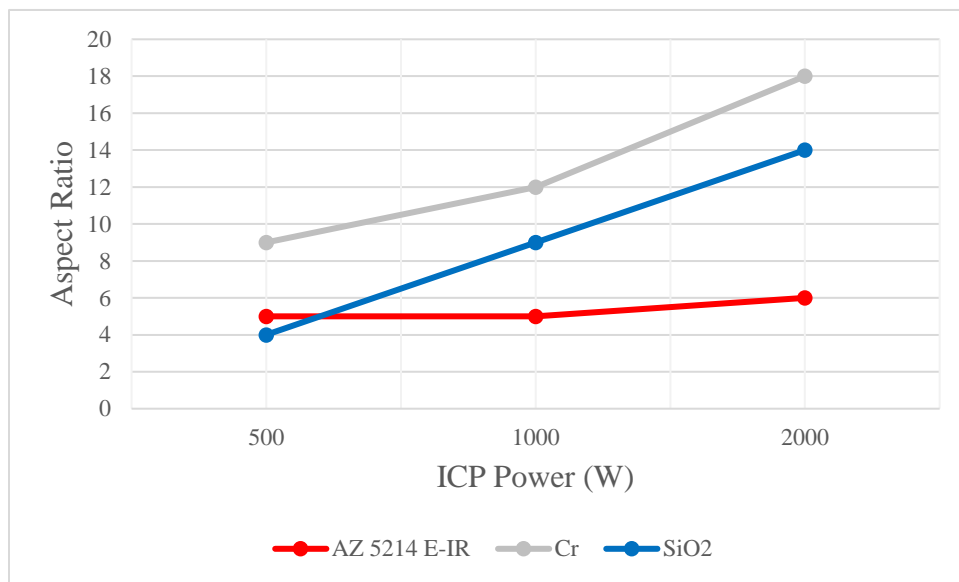


Figure 17: Aspect Ratio vs. ICPP ( $\text{CHF}_3$  gas flow rate = 30 SCCM)

Figure 18 shows how the aspect ratio was measured. The depth of the feature was divided by the width of the feature and that calculation results in the aspect ratio. The yellow cross in this image represents the depth and width measurements.

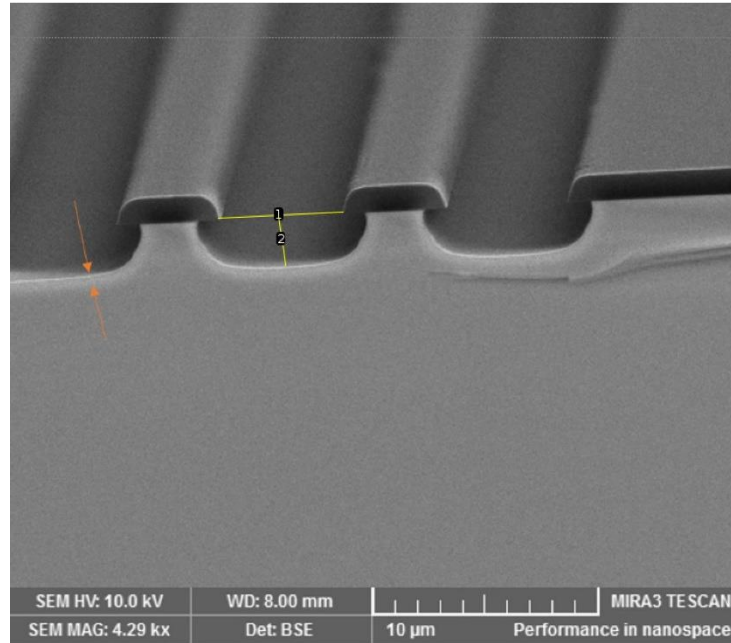


Figure 18: SEM aspect ratio measurements

### 3.4 Effect of CHF<sub>3</sub> Gas Flow Rate

Ideally, the Bosch process uses C<sub>4</sub>F<sub>8</sub> as the process gas during the passivation step because it creates a fluoropolymer layer to protect sidewalls [5]. However, CHF<sub>3</sub> is another type of fluorocarbon gas that is also effective in forming polymers during the passivation step [6]. The Oxford Plasmalab100 ICP RIE at the AggieFab Nanofabrication Facility utilizes CHF<sub>3</sub> as the passivation gas because C<sub>4</sub>F<sub>8</sub> is not an available process gas.

Figure 19 shows the selectivity as a function of the CHF<sub>3</sub> gas flow. The selectivity for both SiO<sub>2</sub> and AZ 5214 E-IR decreased while the gas flow rate of CHF<sub>3</sub> increased. Although CHF<sub>3</sub> forms a carbon layer, the plasma chemistry can also allow it to etch the mask and target materials. A decrease in selectivity for both SiO<sub>2</sub> and AZ 5214 E-IR is a result of an increase in

etch rate for both masks as compared to the etch rate of Si. The Cr etch mask increased in selectivity at 60 SCCM, then slightly decreased at 90 SCCM.

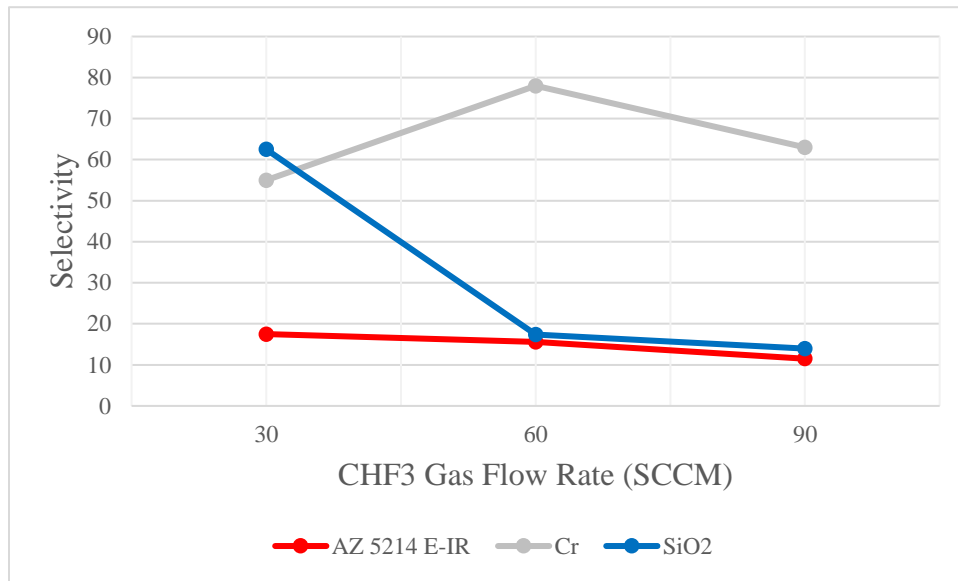


Figure 19: Selectivity vs.  $\text{CHF}_3$  gas flow rate (ICPP = 1000W)

Figure 20 shows the aspect ratio as a function of the  $\text{CHF}_3$  gas flow. All etch mask aspect ratios decreased with an increase in the gas flow rate for  $\text{CHF}_3$ . Increasing the  $\text{CHF}_3$  gas flow generates a thicker layer of passivation on the etch bottom and sidewalls. Thicker passivation layers make it more difficult for the subsequent etch step in the cycle to punch through and continue etching. At these thicker layers, horizontal etching occurred at a faster rate than vertical etching, which decreased the aspect ratio. Figure 21 shows an example of an increase in horizontal etching where an increased amount of Si is being etched under the mask towards the sidewall.

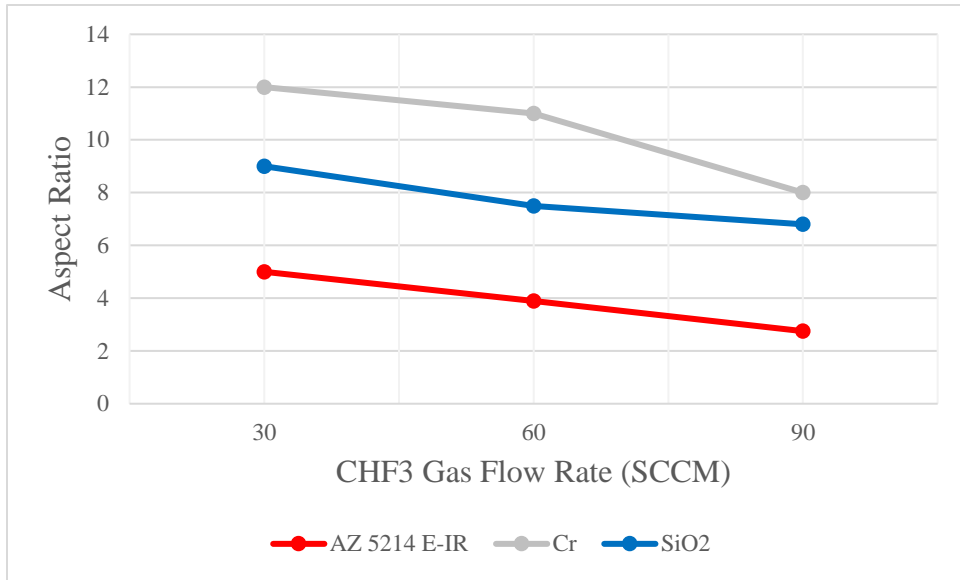


Figure 20: Aspect Ratio vs. CHF<sub>3</sub> gas flow rate (ICPP = 1000W)

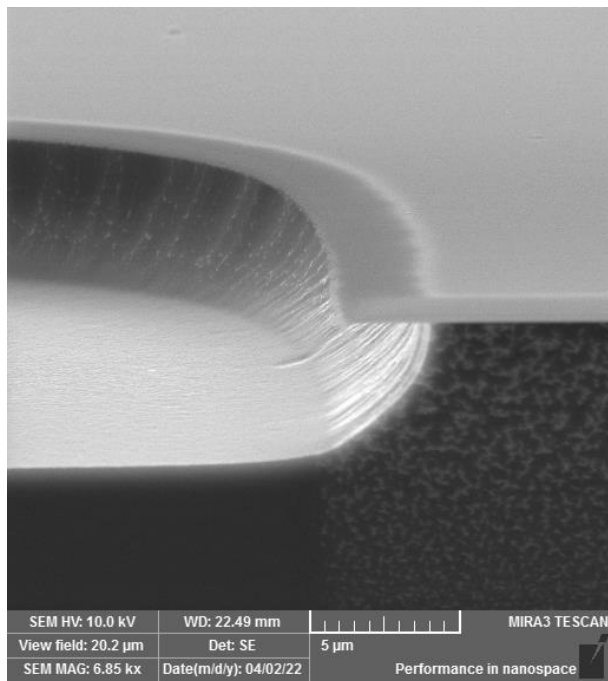


Figure 21: Increased horizontal etching under etch mask

As previously mentioned, punch through, or breakthrough, of the passivation layer is more difficult to achieve at higher  $\text{CHF}_3$  gas flows due to the generation of a thicker passivation layer. If breakthrough of this layer is achieved, then a “scallop” forms on the etch sidewall. This scallop is formed by the bottom of an etch and the beginning of a subsequent etch after breakthrough because passivation tends to coat the sidewalls a lot more than the etch bottom. Thus, Bosch process etch sidewalls usually look like ridges, but they are uniform, nonetheless. These scallops are characteristic of a Bosch process etch. The etches using the Oxford Plasmalab100 ICP RIE were not able to breakthrough the passivation layer, and thus could not create these scallops. Regardless, deep etches were possible on the order of several microns deep.



## 4. CONCLUSIONS

### 4.1 Summary

A DRIE procedure was developed using the Oxford Plasmalab100 ICP RIE at the AggieFab Nanofabrication Facility. Three samples were developed for the testing of different etch masks by using various nanofabrication procedures. These samples were etched by variably changing ICPP and CHF<sub>3</sub> gas flow, and their respective selectivity and aspect ratios were measured.

An increase in ICPP resulted in an increase in selectivity for Cr and SiO<sub>2</sub> due to an increase in the etch rate from greater ion concentration and had no effect on AZ 5214 E-IR photoresist. Aspect ratio for all masks increased regardless of an increase in horizontal/sidewall etching.

Higher CHF<sub>3</sub> gas flows decreased the selectivity for all masks due to an increase in mask etch rate during the passivation step. The aspect ratio for all masks decreased due to the generation of thicker passivation layers.

With the data presented from these tests, future researchers may be able to determine the right parameters necessary for their etches. In addition, the entire sample development workflow for different etch masks is presented along with their respective DRIE results.

### 4.2 Next Steps

Scalloping for this DRIE procedure was not possible. This could be the result of several things. Firstly, Oxford Instruments claims that RIE systems are not capable of performing this technique due to gas restrictions and an imbalance of ions to free radical species. Systems that

can achieve the correct balance are high-density plasma systems (HDP), which also use inductive coupling to generate a plasma [3].

A main restriction in RIE systems is they are not fully suited for immediate gas switching. Since the Bosch process steps cycle so quickly, it is necessary for the tool to be able to perform fast gas switching. Some concerns for the RIE system are that residual SF<sub>6</sub> gas can be left in the chamber even during a CHF<sub>3</sub> passivation step, which can affect etches. The Oxford RIE at the AggieFab Nanofabrication Facility specifically has the gas cabinets connected at about 8-10 feet away from the tool. This is insignificant for most etches but considering fast gas switching is being used for this DRIE procedure, the time it takes for the gas to flow from the tank to the chamber is an impacting factor. For this reason, selectivity will always be lower.

A solution to create scalloping in deep etches that was not explored in these experiments is creating an extra breakthrough step between the etch and passivation steps. The etch step has an RF power of 30 W and the passivation has one at 10 W. A higher RF power can increase vertical etch rates, therefore, a breakthrough step with an RF power of around 50 W could possibly punch through the passivation layer and create deep etches with scalloped sidewalls.

## REFERENCES

- [1.] M. Tilli, V. Lindroos, M. Paulasto-Krockel, S. Franssila, V.-M. Airaksinen, and T. Motooka, Eds., *Handbook of silicon based MEMS materials and technologies (second edition)*. William Andrew Publishing, 2015.
- [2.] SPTS Technologies, “Introduction to Si DRIE,” *SPTS*, 2021. [Online]. Available: <https://www.spts.com/resources/tech-insights/intro-to-silicon-DRIE-etching>. [Accessed: 01-Nov-2021].
- [3.] Oxford Instruments Group, “Deep reactive ion etching (DRIE),” Oxford Instruments, 2021. [Online]. Available: <https://plasma.oxinst.com/technology/deep-reactive-ion-etching>. [Accessed: 18-Oct-2021].
- [4.] A. Ayodele, “Dry etching vs wet etching: Everything you need to know,” *Wevolver*, 14-Dec-2021. [Online]. Available: <https://www.wevolver.com/article/dry-etching-vs-wet-etching-everything-you-need-to-know>. [Accessed: 03-Feb-2022].
- [5.] A. Ayodele, “Dry etching vs wet etching: Everything you need to know,” *Wevolver*, 14-Dec-2021. [Online]. Available: <https://www.wevolver.com/article/dry-etching-vs-wet-etching-everything-you-need-to-know>. [Accessed: 03-Feb-2022].
- [6.] Z. Ouyang, D. N. Ruzic, M. Kiehlbauch, A. Schrinisky, and K. Torek, “Etching mechanism of the single-step through-silicon-via dry etch using SF<sub>6</sub>/c<sub>4</sub>F<sub>8</sub> chemistry,” *Journal of Vacuum Science & Technology A: Vacuum, Surfaces, and Films*, vol. 32, no. 4, p. 041306, 2014.